

1 **Greater host influence and promiscuity: How an invasive seaweed**
2 **host has advantages over co-occurring natives**

3
4
5
6 Marjan Ghotbi ^{1,2}; Guido Bonthond ³; Mitra Ghotbi ⁴; Sven Künzel ⁵; David M Needham ^{1,2};

7 Florian Weinberger ¹

8 ¹GEOMAR Helmholtz Centre for Ocean Research Kiel, 24148 Kiel, Germany

9 ²Faculty of Mathematics and Natural Sciences, Kiel University, 24118 Kiel, Germany

10 ³Institute for Chemistry and Biology of the Marine Environment (ICBM), School of

11 Mathematics and Science, Carl von Ossietzky Universität Oldenburg, Ammerländer

12 Heerstraße 114-118, 26129 Oldenburg, Germany

13 ⁴Department of Biology Middle Tennessee State University, Murfreesboro, USA

14 ⁵Max Planck Institute for Evolutionary Biology, Plön, Germany

15
16
17
18 Marjan Ghotbi <https://orcid.org/0000-0003-4655-6445>

19 Guido Bonthond <https://orcid.org/0000-0002-9823-6761>

20 Mitra Ghotbi <https://orcid.org/0000-0001-9185-9993>

21 David M Needham <https://orcid.org/0000-0001-7257-2516>

22 Florian Weinberger <https://orcid.org/0000-0003-3366-6880>

23

24

25

26

27 Abstract

28 The surface microbiome of seaweed hosts is a multi-domain biofilm regulated by host-microbe
29 and microbe-microbe interactions. The extent to which hosts influence these interactions, and
30 potentially affect their resilience and invasion success, remains unclear. We experimentally
31 tested whether hosts with invasion history exert more influence over their biofilms than native
32 hosts. Biofilm formation on proxy surfaces adjacent to one invasive (*Gracilaria*
33 *vermiculophylla*) and two native (*Fucus serratus*, *Fucus vesiculosus*) co-occurring hosts was
34 monitored and compared to mature epiphytic biofilms of the same hosts. Only *Gracilaria*'s
35 proxy biofilms were significantly different in community composition compared to control
36 surfaces. *Gracilaria*'s proxy biofilms also showed the highest similarity to their adjacent algae
37 sharing certain bacterial taxa that were absent in control treatments, indicating that colonization
38 of the proxy surface was influenced by the host. *Gracilaria* and its proxy biofilm showed
39 highest similarity in microbial network variables, suggesting a higher ability of the invader to
40 influence connectivity and microbial associations within its biofilm. Meanwhile *Gracilaria*'s
41 mature biofilm also showed higher variability in its prokaryotic composition over experiments,
42 which was also reflected in a less robust microbial network in both *Gracilaria* and its proxy
43 biofilms. This suggests that in addition to stronger influence in the invasive host, it was also
44 more promiscuous towards potential symbionts from the environment. Ultimately, through
45 examining microbial interactions, in line with previous research we found that host influence
46 and promiscuity may play an important role in seaweed hosts to acclimate to different
47 environmental condition and successfully thrive in new ecosystems.

48

49 Keywords: Multi-domain Biofilm; Seaweed Holobiont; Core Microbiome; Hub Taxa;
50 Microbial Community Resilience; Invasion Success; Microbial Connectivity, Microbial
51 Network

52

53

54 Introduction

55 Host-microbe and microbe-microbe interactions play a crucial role in establishing a robust
56 microbial community of a holobiont. These interactions are affected by metabolite exchange,
57 signalling, and physiochemical changes [1, 2]. Structural features of the seaweed microbiome
58 as a multi-domain biofilm give it a distinctive influence on shaping these interactions. Presence
59 of microenvironments with different osmolarity, nutrient availability, gas concentrations, and
60 cell density of heterogeneous microbial communities stimulates the formation of three-
61 dimensional structures within biofilm [3], which supports intercellular communication, nutrient
62 acquisition, and protection of the microbial community [4]. While primary metabolites are
63 recognized as inducers of microbial colonization [5], different hosts harbour distinct microbial
64 communities [6, 7], which can occur due to host-specific signals. Some seaweeds reportedly
65 have the ability to recruit protective bacteria and deter pathogens through secretion of surface
66 metabolites [1]. Investigating these recruitment processes will further our understanding of how
67 interactions between seaweeds and environmental microbiome, and also between recruited
68 microbes determine the final biofilm composition and connectivity, and how these interactions
69 influence resilience, dispersal and invasion success of seaweeds.

70

71 Members of the brown algal genus *Fucus* (Phaeophyta) are important habitat forming species
72 in many shallow water regions of the northern hemisphere and especially in the Baltic Sea [8].
73 *Fucus vesiculosus* and *Fucus serratus* are two co-occurring species [9] in the littoral zone [8].
74 During the last five decades, populations of these two species in the Baltic Sea have been
75 negatively affected by several biotic and abiotic stressors, in particular increased
76 eutrophication, sedimentation, grazing pressure [8, 10–13], warming and seasonal variability
77 [14]. In contrast, *Gracilaria vermiculophylla* is an invasive habitat-forming red alga
78 (Rhodophyta) that also co-occurs with the two *Fucus* species in the Baltic Sea [15] and has
79 successfully invaded many *Fucus* habitats despite the given threats. *G. vermiculophylla* is
80 native to the Northwest Pacific, and has a wide invasive distribution in the Eastern Pacific [15],
81 Eastern Atlantic including the Baltic Sea [16] and Western Atlantic [17]. There is evidence that
82 host-microbe interactions have played a crucial role in the invasion process of
83 *G. vermiculophylla* [1, 18]. Invasive *G. vermiculophylla* populations, compared to natives, have
84 high host promiscuity (flexibility toward potential symbionts from the environment) [19] and
85 exert more influence over their epibiota [20]. This enhanced influence was associated with
86 better host performance under thermal stress, indicating it may importantly contribute to the
87 capacity of a seaweed host to acclimate to new environments [20]. Also, co-introduction of
88 core-microbes that provide essential functions to the host across its distribution range has been
89 suggested to facilitate the invasion process (reviewed by [18]).

90

91 Complex host-microbe and microbe-microbe interactions within seaweed biofilms, their role in
92 ecological success of the host, [21], and the observed shifts in the populations of the three
93 macroalgal species, prompted us to study and compare how these hosts recruit microbes from
94 the environment and influence microbial composition, interactions and connectivity in their
95 biofilm. To this end, we used sterile, inert, porous artificial surfaces (polycarbonate filters of

96 0.22 μm pore size) in close proximity to the seaweed species without direct contact to provide
97 substrate for biofilm formation, hereafter referred to as Proxy Biofilm (PB). This method helped
98 to isolate the influence of exudates while eliminating other sources of variation in biofilm
99 colonization such as host morphology [22], physical properties [23], priority effects (impact of
100 an already established community)[24], as well as environmental factors [25, 26] which were
101 consistent across species as they were all deployed in the same habitat. The developing proxy
102 biofilms were then used to evaluate the hosts influence on colonization through exudates
103 production, and were compared with mature biofilms on seaweed specimens over two
104 experiments of different durations.

105

106 Based on the hypothesis that *G. vermiculophylla* exerts stronger host influence compared to the
107 native *Fucus* species, we tested two sub-hypotheses; i) PBs of the invasive seaweed host are
108 more distinct from control filters, and ii) these PBs are more similar to the host mature biofilm
109 in terms of diversity, composition, and microbial connectivity compared to BPs of the two
110 native hosts. We also hypothesized that *G. vermiculophylla* has higher host promiscuity,
111 allowing more flexibility toward potential symbionts and more resilience of the biofilm to
112 changes in the environment. Here, we also tested two sub-hypotheses; iii) the mature biofilm
113 of invasive hosts shows short-term temporal variation in diversity and/or composition and iv)
114 microbial connections on the invasive host and its PBs are less stable with higher propensity
115 for reconnection compared to natives.

116

117 Materials and Methods

118 2.1. Algae collection and experimental setup

119

120 The three seaweed species *F. serratus*, *F. vesiculosus*, and *G. vermiculophylla* were collected
121 on 20 October 2020 from two sampling sites, Falckensteiner Strand (54°23'37.3" N,
122 10°11'16.9" E) and Bülk (54°27'15.0" N, 10°11'50.6" E). Six intact specimens of each species
123 with comparable size were taken from each site. After an acclimation period of two weeks,
124 seaweed species were cleaned from foulers, and approximately similar biomass of the species
125 (Tab.S1-metadata) was transferred into the experimental setup. Our setup, EXUTAX (Fig.1),
126 attached to the Kiel Outdoor Benthocosms (KOB) [27], was designed to capture the impact of
127 host exudates (EXU) on microbial chemotaxis (TAX) and biofilm formation. We used 47 mm,
128 0.22 µm Nuclepore Polycarbonate Black Membrane Filters (GVS Life Sciences, Italy) as
129 substrates for PB formation. Environmental data were collected autonomously at two-minute
130 intervals for the appropriate depth of the setup from continuous measurements at the Kiel Fjord
131 GEOMAR Pier (available on PANGAEA, average values reported in Tab.S1).

132

133 2.2. Proxy biofilm formation, sample collection and processing

134

135 Two EXUTAX experiments were conducted in November and December 2020. In the first
136 experiment, samples of the seaweed biofilms, PBs and control were collected on day seven
137 (experiment spanned 3rd to 10th November), and in the second experiment on day 14 (18th
138 November to 1st December). For the isolation of algal biofilm, approximately one g of each
139 algal sample was taken and transferred to a tube containing sterile glass beads in 15 ml of
140 artificial seawater. Bead beating was used to dislodge the biofilm from the seaweeds [18]. At
141 both timepoints, 200 mL of ambient seawater was filtered on to a 0.22 µm polycarbonate filter.
142 For studying the collected PBs, we used a combination of microscopy and molecular
143 techniques. 1/8 of each filter was cut for enumeration via epifluorescence microscopy

144 (supplementary information), and the rest was immediately submerged in 2% CTAB isolation
145 buffer for DNA extraction.

146

147 2.3. DNA extraction and 16S rRNA gene sequencing 148

149 DNA from all biofilms was extracted following a DNA isolation Protocol for Plants [28]. The
150 16S-V4 region was amplified with the primers 515F (S-*-Univ-0515-a-S-19) and 806R (S-D-
151 Arch-0786-a-A-20), as in [18, 29], and sequenced via 2×300 bp reads on Illumina MiSeq.
152 Adapters were removed from raw sequence reads with cutadapt [30]. Forward and reverse reads
153 were truncated at 220 and 200, respectively, and processed via default settings with DADA2
154 [31] in QIIME 2 2022.11 [32]. Amplicon sequence variants (ASVs) were classified via q2-
155 feature-classifier [33] against the SILVA 138.1 database [34]. Subsequently, for the prokaryotic
156 dataset, chloroplast, mitochondria, and samples less than 2000 reads were removed and gene
157 copy numbers corrected via q2-gcn-norm (2021.04) based on rrnDB database (v. 5.7) [35, 36].
158 For the microalgae dataset, chloroplasts first identified by SILVA, were additionally classified
159 with the PhytoRef database [37, 38], and samples with less than 100 reads were removed.
160 Unassigned ASVs were reclassified when possible, using a phylogenetic approach that helps
161 with classification of mitochondria and chloroplast (supplementary information) (Tab.S2-A;
162 Tab.S2-B).

163

164 2.4. Identification of core microbiome and host influence

165

166 To evaluate host influence in attracting and maintaining specific groups of persistently
167 associated taxa, we characterized a compositional core [39–41] at phylogenetic and short term
168 temporal scale for both algae and PBs. ASVs with > 3 sequence reads, detected in at least 90
169 percent of each sample group, were considered members of the corresponding compositional

170 core. A very low abundance threshold (0.001%) was specified to capture microbes even with
171 rare representation in the community, since they might be physiologically more active
172 compared with more abundant ones [39, 42]. In addition, to capture host specificity, we detected
173 ASVs present in 100% of each seaweed species and their corresponding PBs across both
174 experiments, but absent in control filters and seawater samples.

175

176 2.5. Microbial association network construction

177

178 To evaluate cross-domain associations (significant abundance correlation between and within
179 prokaryotes and microalgae), SPIEC-EASI network analyses [43] were applied at both the
180 whole microbial community (WMC) and core microbiome (section 2.4) levels on merged ASV
181 datasets of seaweeds, and PBs including control samples (supplementary information). For
182 WMC, ASVs with < 3 reads and $< 0.25\%$ minimum relative abundance were excluded (this
183 abundance threshold was used since it was the minimum required for *Fucus* hosts networks to
184 reach stability). Hub taxa, module (a cluster of interconnected microbes) and network hubs,
185 were identified for each sample group based on within- and among-module connectivity [44,
186 45].

187

188 2.6. Statistical analysis

189 2.6.1. Diversity and quantification

190

191 Linear mixed models (LMM) [46] from the R package lme4 were used to estimate the
192 comparative and interactive effects of seaweed exudates on prokaryotic and microalgal
193 diversity (Shannon indices) on both living (mature biofilm) and non-living (polycarbonate
194 filter) substrates across two experiments. LMM was also applied to evaluate the impact of

195 seaweed exudates on the enumerated values of microalgae. Seaweed exudate impact on mature
196 biofilm (n=33) and PBs (n=35) and timepoint were considered as fixed factors. The factor panel
197 was included as random effect to account for non-independence among observations from
198 bottles installed on the same panel and the factor bottle to account for non-independence
199 between filters and seaweeds from the same bottle over two experiments.

200

201 2.6.2. Community composition

202

203 Variability in microbial composition was analysed using permutational analysis of variance
204 (PERMANOVA) with Bray-Curtis distance matrices, after testing for homogeneity of
205 dispersion (beta dispersion), through vegan package [47] with 999 permutations. ANCOM-BC
206 [48] was used to find differentially abundant ASVs (at phylum level) in *G. vermiculophylla*
207 mature biofilm between two experiments.

208

209 2.6.3. Microbial connectivity

210

211 To identify similarity between microbial connectivity in distinct biofilms, we generated a
212 Euclidean distance-based analysis using mean values of network variables calculated from
213 significant connections detected in each network which visualized through PCA and heatmap.

214

215 Results

216 3.1. Microbial community composition across seaweed biofilms and PBs

217

218 The prokaryotic community analysis, after processing, had 12,685 ASVs and 2,431,184 reads
219 across 87 samples (36 seaweeds, 35 PBs and 14 control filters, and two ambient water).
220 Seaweeds had the highest number of unique ASVs (2655) followed by PBs and control filters
221 (1074) and 179 ASVs were shared between all samples (Fig.S1-A). The microalgae dataset (via
222 chloroplasts) had 187 ASVs and 827,700 reads across 84 samples (33 seaweeds, 35 PBs and 14
223 controls, and two ambient water). PBs and control filters had the highest number of unique
224 microalgal ASVs (73) vs. seaweeds (18) and 25 were shared between all (Fig.S1-B).

225
226 Across all surfaces (seaweeds, PBs, and control filters), Proteobacteria was the most abundant
227 phylum, followed by Bacteroidota and Planctomycetota. However, in ambient water,
228 Crenarchaeota was the second most abundant phylum after Proteobacteria (Fig.S2-A).
229 Desulfobacterota and Campylobacterota phyla were mainly associated with seaweed samples,
230 with higher abundance on *G. vermiculophylla*. Firmicutes and LCP-89 showed high relative
231 abundance exclusively in the *G. vermiculophylla* biofilm, while Spirochaetota and
232 Acidobacteriota were more abundant in *Fucus* species. The microalgae community on all
233 surfaces was strongly dominated by Bacillariophyta, while in ambient water it consisted of
234 Bacillariophyta and Cryptophyceae (Fig.S2-B).

235 Analysis of the 30 most abundant prokaryotic ASVs showed higher abundances of
236 *Spongibacter*, *Neptomonas* and *Desulforhopalus* on the *G. vermiculophylla* biofilm and its PBs
237 (Fig.2-A). *Fucus* species and their PBs showed higher abundance of ASVs from the BD1-7
238 clade (specifically ASV1404), however, *G. vermiculophylla* biofilm and its PBs were almost
239 devoid of this ASV (Fig.2-A). Generally, PBs and control filters were enriched with
240 Alphaproteobacteria. Among microalgae, ASVs belonging to Melosiraceae,
241 Coscinodiscophyceae, Cymbellaceae, Bacillariophyceae were strongly associated with
242 surfaces. However, Thalassiosirales and Pyrenomonadales were mainly found in ambient water.

243 Some members of the Cymbellaceae family showed degrees of host specificity. For instance,
244 ASV125 was consistently associated with *G. vermiculophylla* and not detected among abundant
245 ASVs of other samples, while ASV81 and ASV154 were primarily detected on *Fucus* species
246 and not among the abundant ASVs of PBs (Fig.2-B).

247

248 3.2. Microbial profiling and quantification

249

250 In both experiments, prokaryotic diversity (Shannon indices) exhibited no significant
251 differences between control filters and *G. vermiculophylla*'s PBs, and generally diversity stayed
252 similar across all treatments on non-living substrate (Fig.3-A; Tab.S3-B). Only diversity of
253 *G. vermiculophylla*'s PBs was similar to their corresponding algal treatment and native hosts
254 showed significant differences with their PBs (Fig.3-B). The highest prokaryotic diversity was
255 observed in the mature biofilm of *Fucus* algae, and their Shannon indices were significantly
256 higher compared to *G. vermiculophylla* and to PBs (Fig.3-B). While diversity on non-living
257 substrates was significantly higher during the second (longer) experiment (Tab.S3-B), no
258 significant change over time was observed on mature algae biofilms (Tab.S3-C; Fig.3-C).
259 Likewise, microalgae diversity also stayed similar on non-living substrates across all algal
260 treatments, and no significant differences were detected between control filters and
261 *G. vermiculophylla*'s PBs (Fig.3-D). All algae and their PBs showed similar diversity over both
262 experiments (Fig.3-E) and the only difference was seen among substrate types, primarily in the
263 second experiment (Tab.S3-D). Enumeration of microalgae observed on PBs and control filters
264 (n=47) except for between two experiments, did not show any significant difference between
265 algal treatments and control (Fig.S3; Tab.S4).

266

267 The prokaryotic community on seaweeds biofilm was fully separated by PCoA from that on
268 PBs along the first principal component axis PCoA1, while PCoA2 mainly separated the
269 biofilm of two algae genera (Fig.4-A). The PERMANOVA likewise detected significant impact
270 of living and non-living substrate (seaweed vs. PBs; $R^2=0.18$, $p=0.0001$; Tab.S5-A). The
271 prokaryotic community on non-living substrate (n=49) showed significant impact of algal
272 treatments. Pairwise ADONIS detected only a significant difference between PBs of
273 *G. vermiculophylla* and control filters ($R^2=0.06$, $p=0.048$; Tab.S5-B). Pairwise ADONIS on
274 algae mature biofilms (n=36) showed a significant difference of *G. vermiculophylla* and the
275 two *Fucus* species (Tab.S5-C). All developing biofilms on non-living substrates and only
276 *G. vermiculophylla*'s mature biofilm (n=12) exhibited significant shifts of prokaryotic
277 communities over time as an influence of environmental changes (Tab.S5-B,C). Observed
278 environmental data over the two experiments showed differences in salinity, temperature,
279 oxygen saturation levels and irradiation, with temperature in *G. vermiculophylla*'s BP and
280 mature biofilm as well as salinity (conductivity) in all non-living substrate samples being the
281 main source of variation (Tab.S.6-A:C). Microalgal communities also mainly differed between
282 substrates, as indicated by the separation along PCoA1 (Fig.4-B), and detected by
283 PERMANOVA (n=82; $R^2=0.19$, $p=0.0001$; Fig.4-B; Tab.S5-D). The microalgal communities
284 on seaweed surfaces (n=33) showed a significant difference between *G. vermiculophylla* and
285 the two *Fucus* species (Tab.S5-F), consistent with patterns observed in the prokaryotic
286 community. Microalgae showed a significant shift over time on both substrates suggesting an
287 impact of environmental factors (Tab.S5). In contrast to the prokaryotic community, the
288 presence of different seaweed treatments had no significant effect on the microalgal community
289 on non-living substrates (Tab.S5-E).

290

291

292 3.3. Core microbiome

293
294 *G. vermiculophylla*'s biofilm showed the highest ASV and phylum level diversity in its
295 prokaryotic core microbiome, with 175 ASVs vs. 148 for *F. vesiculosus*, and 94 for *F. serratus*
296 (Fig.S4). Members of two *Fucus* species shared a higher number of their core ASVs compared
297 to *G. vermiculophylla*. Core taxa of PBs compared to seaweeds showed higher diversity at ASV
298 but lower at phylum level. PBs showed the same trend among seaweed species with 191, 189
299 and 137 ASVs correspondingly. Controls possessed the lowest diversity of ASVs (93) and
300 phyla within their core (Fig.S4; Tab.S7-A). Although the differences were not statistically
301 significant, they highlight *G. vermiculophylla*'s potential for maintaining a broader range of
302 prokaryotic diversity in its core taxa. The microalgae core taxa were generally lower in numbers
303 compared to prokaryotes (Fig.S4). Likewise, PBs showed higher diversity of ASVs compared
304 to seaweeds (Fig.S4; Tab.S7-B). Two prokaryotic ASVs, identified as Rhodobacteraceae and
305 *Granulosicoccus*, were present in 100% of the *G. vermiculophylla*'s biofilm and its PBs, but
306 were rarely and in very low abundances detected in other seaweed samples and absent from
307 other proxy biofilms. Presence of these host-specific ASVs denotes higher similarity between
308 *G. vermiculophylla*'s biofilm and PB, suggesting stronger influence of *G. vermiculophylla*'s
309 exudates in attraction of specific bacteria in the environment (Tab.S7-A).

310

311 3.4. Microbial association network

312
313 The WMC of *Fucus* species showed the most similarity (Fig.5-A) and were strongly separated
314 from *G. vermiculophylla* and PBs, consistent with diversity results. PBs were distinct from
315 control biofilms mainly in core microbiomes (Fig.5-A,B). The most dissimilarity between PBs
316 and control filters was seen in the core microbiome of *G. vermiculophylla*. In terms of microbial
317 connectivity, the most similarity between seaweeds and their PBs was seen in

318 *G. vermiculophylla* for both WMC and core microbiome (Fig.5-A,B). Conversely, the most
319 dissimilarity was seen in *Fucus* species and their PBs in both WMC and core microbiome
320 (Fig.5-A,B).

321
322 Beyond the broad overview of similarities, in terms of various individual metrics, microbial
323 networks showed opposite trends at WMC vs. core microbiome of each seaweed (Fig.5-C,D).
324 First, among WMCs, the sparsest network was seen in *G. vermiculophylla* mature biofilm with
325 the lowest average number of connections between nodes or ASVs (mean degree) compared to
326 *Fucus* species (Fig.5-C; Tab.S8). However, between core microbiomes, *G. vermiculophylla* and
327 its PBs had among the highest number of connections, along with *F. serratus* PBs (Fig.5-D).
328 Relatedly, the robustness of the networks as a function of natural connectivity [49], was lowest
329 for the WMC of *G. vermiculophylla* mature biofilm; however, its core microbiomes of both
330 mature biofilm and PBs showed among the highest corresponding values after *F. serratus*
331 mature biofilm (Fig.5-C,D). The clustering coefficient (fraction of observed vs. possible node
332 clusters) which represents the complexity of the network due to strong interactions among
333 microorganisms [50, 51], also showed the same trend between the *G. vermiculophylla*'s WMC
334 to its core microbiome, with *G. vermiculophylla*'s core on both mature biofilm and PBs
335 showing the highest network complexity (Fig.5-C,D; Fig.6). The highest modularity, denoting
336 denser connections between the nodes within modules but sparse connections between nodes
337 of different modules [45, 51], was observed in the WMC of *Fucus* species than
338 *G. vermiculophylla* (Fig.5-C). While the highest modularity of WMC in algae mature biofilm
339 was with *F. serratus*, its core microbiome showed the lowest value (Fig.5-C), which denotes
340 presence of less stable niches in its core taxa. Among core microbiomes, frequencies of
341 associations and specifically negative associations were significantly lower in *Fucus* species
342 (Fig.6).

343

344 Regarding the taxonomic membership, the networks of WMC of seaweeds biofilms consisted
345 of nodes from three microbial domains including prokaryotes (bacteria, archaea) and
346 eukaryotes (microalgae). Regarding bacteria, *G. vermiculophylla* possessed the highest number
347 of nodes from *Desulfobacterota*, with the *Desulforhopalus* accounting for the highest degree
348 (number of connections) and betweenness (centrality). However, *Fucus* species possessed
349 higher abundance and diversity of Proteobacteria, Bacteroidota and Planctomycetota. For
350 archaea, *Fucus* species as well as PBs had *Nitrosopumilus* (shared with ambient water) (Fig.S5-
351 A:B), while *G. vermiculophylla* possessed two archaeal ASVs as *Methanolobus*, a
352 psychrophilic methanogen and SCGC_AAA286-E23 (candidate phylum Woesearchaeota)
353 (Fig.S5-C; Tab.S9). SCGC AAA286-E23 is reported as anaerobic [52] symbiont of other
354 prokaryotes [52–54]. Higher among-module connectivity of this archaeon, as a connector node
355 (a node connecting within and between microbial sub communities [45]), supports its symbiotic
356 lifestyle (Tab.S9). In all seaweed's mature biofilm, dominant contributors of microalgae
357 community were Stramenopiles (Bacillariophyta). *G. vermiculophylla* in addition, had a
358 representative from Archaeplastida (Coccomyxaceae) with relatively high betweenness and
359 degree (Fig.S5-C; Tab.S9). ASV125 (Cymbellaceae) which was only detected in high
360 abundance on *G. vermiculophylla* (Fig.2-B) and classified as a connector node (Tab.S9) was in
361 the same module with *Methanolobus* and sulfur cycle bacteria (Fig.S5-C), suggesting potential
362 metabolic interactions among these microbes.

363

364 In the network of core microbes, 46 ASVs and three associations were shared between
365 *G. vermiculophylla* and its PBs, five of which were not detected on control filters (Tab.S10). In
366 particular these three associations were between Rhodobacteraceae with *Eudoraea*,
367 *Sulfitobacter* with *Sulfitobacter*, and Hyphomonadaceae with Flavobacteriaceae (Fig.7).

368 *F. vesiculosus* and *F. serratus* shared 50 and 26 ASVs with their PBs networks, but no
369 associations (Tab.S10). However, with the exception of two ASVs in *F. vesiculosus* all were
370 shared with control filters (Tab.S10). To examine the individual taxa that could have outsized
371 roles in maintaining connectivity and functioning of the network, we analyzed ‘hub taxa’, which
372 are a small number of strongly interconnected microbes [45, 55]. Hub taxa for different
373 seaweeds and PBs were defined based on within-module and among-module connectivity of
374 nodes within each network [44, 56]. *Sulfitobacter* (Alphaproteobacteria), and P3Ob-42
375 (Myxococcota) were identified as hub taxa for *G. vermiculophylla*. OM190, *Phycisphaera*,
376 *Blastopirellula* (Planctomycetota), *Lutimonas* (Bacteroidota), and *Nannocystis* (Myxococcota)
377 composed hub taxa of *F. vesiculosus*. *F. serratus* hosted ASVs from Rhodobacteraceae
378 (Alphaproteobacteria), *Colwellia* (Gammaproteobacteria), Arcobacteraceae
379 (Campylobacterota), Planctomicrobium (Planctomycetota), Cryomorphaceae, Saprospiraceae,
380 *Wenyngzhuangia* (Bacteroidetes) as its hub taxa (Fig.S7; Tab.S11).

381

382 Discussion

383 4.1. Host influence on microbial composition and interactions in its biofilm

384

385 The ability of hosts to influence the biofilm composition can potentially aid their dispersal
386 across diverse environments, contributing to invasion success [20]. Using an *in-situ* approach,
387 we found that the invasive alga (*G. vermiculophylla*) expressed more host influence over its
388 biofilm and more promiscuity toward potential symbionts and their interactions, compared to
389 the native species (*F. serratus* and *F. vesiculosus*). *G. vermiculophylla* caused significant
390 difference between its PBs and control filters composition (Tab.S5-B). This invasive alga also
391 showed higher similarity between its mature biofilm and PBs regarding terms of diversity

392 (Tab.S3-A), and microbial connectivity (Fig.5) which suggests that the host influenced the
393 microbial community on the PBs at a structural level. Further, more microbial taxa, including
394 host-specific taxa (Fig.7) were shared between *G. vermiculophylla* and its PBs, compared to
395 *Fucus* species. This supports the first and second hypotheses, highlighting the invasive host's
396 stronger host influence on its PBs. This influence is likely driven by host-produced exudates,
397 exchanged through the PB filters, which may attract and/or deter environmental microbes [1].
398 A positive association between Hyphomonadaceae and Flavobacteriaceae was seen on
399 *G. vermiculophylla*. Both families have been recurrently reported on *G. vermiculophylla* and
400 other macro [57–59] and microalgae [60]. Additionally, two ASVs of Rhodobacteraceae and
401 *Granulosicoccus* showed high degrees of host specificity and were exclusively shared between
402 *G. vermiculophylla* and its PBs. These taxa were reported to be among winter core microbiome
403 of *G. vermiculophylla* [59]. Members of the Rhodobacteraceae family are known for
404 association with initial surfaces colonization in marine ecosystems due to their ability to react
405 to low levels of nutrients faster than other bacteria [61]. Hence these bacteria may be among
406 the initial colonizers of *G. vermiculophylla* with influence on community succession.
407 *Granulosicoccus*, a flagellated bacterium capable of chemotaxis [62], is one of the rare
408 Gammaproteobacteria that encode a DMSP demethylase, widely found in marine
409 Alphaproteobacteria [62, 63]. Epiphytic *Granulosicoccus* also has been reported to carry
410 metabolic genes for nitrate and nitrite reduction [62], sulfur transformation [64], and vitamin
411 B-12 production [64], suggesting critical roles for this genus in nutrient cycling and vitamin
412 acquisition for both the auxotrophic host and its biofilm assembly.

413

414

415 4.2. Distinct biofilm connectivity and microbial associations on invasive and native hosts

416

417 Invasive and native seaweeds supported distinct microbial diversity and communities. Their
418 networks of association also differed between WMC and core microbiomes. Algal PBs had
419 similar communities and diversity but differed in microbial association networks. The WMC
420 of *G. vermiculophylla* mature biofilm demonstrated the lowest robustness (lower mean degree
421 and natural connectivity) and at the same time the highest density of connections (number of
422 present connections to all possible connections) which can potentially denote flexible
423 reassembly and thus high host promiscuity, which supports our third and fourth sub-hypothesis
424 that *G. vermiculophylla* is more promiscuous toward potential symbionts. This host trait may
425 importantly promote acclimation to changing environmental conditions. This was also
426 supported by the networks of *G. vermiculophylla*'s PBs which revealed less stable microbe-
427 microbe connectivity compared to *Fucus* BPs (Fig.5), suggesting the invasive host is less
428 dependent on the WMC community. In contrast to WMC, the core microbiome of
429 *G. vermiculophylla*, on both mature biofilm and PBs, possessed a higher number of connections
430 (edge density), and showed stronger associations and more developed and complex
431 connectivity compared to core taxa of *Fucus* species (Fig.6). This suggest that while
432 *G. vermiculophylla*'s biofilm is generally flexible toward environmental microbes, it
433 persistently maintains a diverse and interconnected core community. Unlike
434 *G. vermiculophylla*'s WMC, its core microbiome exhibited a higher clustering coefficient in
435 both mature biofilm and PBs (Fig.5-C,D), indicating a greater potential for niche
436 differentiation. This theoretically facilitates coexistence of diverse core microbial taxa by
437 reducing direct competition [65], which aligns with our findings on higher diversity in
438 *G. vermiculophylla*'s core taxa (Tab.S7-A). Presence of functionally developed microbial
439 subcommunities within the core microbiome of *G. vermiculophylla* may aid with nutrient
440 acquisition and defence. Contrarily, the *F. serratus* biofilm with the highest prokaryotic
441 diversity in its WMC revealed the most depauperate core microbiome. *F. serratus* core taxa,

442 while displaying the highest connectivity relative to their number, showed the weakest
443 associations (Fig.5-D; Fig.6). Generally, *Fucus* species and specifically *F. serratus*, showed
444 weaker microbe-microbe associations within their core microbiome niches (Fig.6). This
445 denotes less stability of functional groups within *Fucus* species core microbial taxa.

446
447 Networks of *G. vermiculophylla*'s biofilm, both in WMC and core, possessed the highest
448 number and diversity of *Desulfobacterota*, the largest phylum harboring sulfate-reducing
449 bacteria (SRB) [66], with *Desulforhopalus* ASVs having an intermediary role in facilitating
450 connections between other taxa. Members of the Desulfocapsaceae family exhibit diverse
451 phenotypic characteristics, such as a wide temperature tolerance, different motility properties,
452 anaerobic chemolithotrophic or chemoheterotrophic metabolism, and utilization of various
453 electron donors and acceptors for sulfate reduction, which helps them to thrive under different
454 environmental conditions [66]. Presence of this taxonomic guild in high abundance can
455 contribute to resilience of the host biofilm and its function under different environmental
456 conditions. Seaweed hosts and their associated microalgal community usually provide a
457 substantial quantity of organosulfur compounds that can be degraded by bacteria [67].
458 Numerous bacteria produce extracellular enzymes that require suboxic or anoxic environments
459 to support microaerophilic or anaerobic metabolism. Anaerobic microniches formed in biofilms
460 could facilitate this [68], and enhance nutrient cycling that benefits their hosts. An increase in
461 the relative abundance of certain anaerobic prokaryotes including symbiotic Woese archaeota
462 [52–54], along with aerotolerant anaerobic Cloacimonadota [69] in the *G. vermiculophylla*
463 biofilm in the second experiment (Fig.S6) implies the presence of microniches influenced by
464 host rather than direct impact of environment. Sulfate availability in anoxic environments can
465 facilitate DMS degradation by methanogens and SRB [70]. The positive association between
466 sulfur cycling bacteria and methanogenic archaea (Fig.S5-C), suggests presence of such

467 syntrophic relationship between these groups within the *G. vermiculophylla* biofilm similar to
468 what has been observed in anoxic sediments [70].

469

470 Hub taxa, have been reported to be able to reflect controlling impact of the host genotype on
471 microbiome assembly [55]. In short, the environment directly affects “hub” microbes, and this
472 effect transmits to the microbial community via microbe–microbe interactions [55]. P3Ob-42
473 (Myxococcota phylum) was identified as most central hub taxon of *G. vermiculophylla* with
474 the highest connectivity within and between subcommunities (Tab.S11; Fig.S7). P3Ob-42 is a
475 potential sulfate reducer and methane oxidizer and contributes to nitrogen and phosphate
476 cycling [71]. It is reported to be associated with good health status of marine hosts, specifically
477 Carrageenophyte red algae and corals [72, 73]. *Sulfitobacter*, the second hub taxon of
478 *G. vermiculophylla* (Fig.S7), is known for its potential DMSP degradation, growth promoting
479 impact and contribution to the health of algae and corals in cold marine environments [72, 74,
480 75]. Hub taxa in *F. serratus* included Planctomycetota, Bacteroidota, and Campylobacterota.
481 *F. vesiculosus* also included Bacteroidota but was dominated by hub taxa from Planctomycetota
482 (Fig.S7). *Fucus* spp. secrete fucoidan, a sulfated polysaccharide, containing high percentages
483 of L-fucose and sulfate ester groups [76], that serve as a substrate for the abundant sulfatases
484 produced by Planctomycetota and favour their colonization [77]. In addition, The
485 peptidoglycan-free cell wall of most Planctomycetota enables resistance to antimicrobial
486 activities from host and other bacteria in the biofilm [77].

487

488 4.3. Greater acclimation potential of invasive host’s biofilm to environmental changes

489

490 Prokaryotic community composition in *G. vermiculophylla*’s mature biofilm showed a
491 significant shift over time (Tab.S5-C). This shift may be driven by environmental changes,

492 including water temperature, salinity, oxygen levels and irradiation impacting host [78] and
493 hence its biofilm during the second experiment (Tab.S1; Tab.S6-A). This observation is an
494 additional support to the third hypothesis that the invasive holobiont is more promiscuous and
495 can undergo greater shifts in its biofilm composition over time [19]. The host promiscuity was
496 also supported by less robust microbial networks in both *G. vermiculophylla* and its proxy
497 biofilm. Host promiscuity may enable a host to associate a taxonomically or compositionally
498 different microbiome, which maintains functions essential to the host [79]. This may be an
499 important trait for seaweeds, facilitating acclimation and potentially supporting biological
500 invasions [19]. Whereas previous work on *G. vermiculophylla* showed that host promiscuity
501 varies between native and invasive populations of the same species [19], this study provides
502 evidence that host promiscuity also varies between invasive and native species co-existing in
503 the same environment that can impact their competitions and ecological success.

504

505 5. Conclusion

506 While previous work has found that invasive *G. vermiculophylla* populations have greater host
507 influence [20] and promiscuity than its native populations [19], this study is the first to compare
508 invasive versus native hosts of different species coexisting in the same environment using an
509 *in-situ* experiment isolating the impact of exudates from the host substrate itself. It is also the
510 first study to look specifically at microbial interactions of the given hosts, providing a new layer
511 of evidence on how host influence and promiscuity at the level of microbe-microbe interactions
512 may drive seaweeds invasions. In addition, we found stronger host-microbe and microbe-
513 microbe associations within a set of conserved core microbes associated with
514 *G. vermiculophylla*, despite its higher host promiscuity. This suggests that some taxa fulfil key
515 functions and are not easily replaced, and may have accompanied their host through the

516 invasion process. Although some of these taxa were recruited in the new environment, further
517 research is needed to unravel the native or invasive origin of these specific symbionts.
518 Ultimately, our results suggest that host influence plays an important role in seaweed
519 holobionts. While the exact identity of exudates remains unknown, this study demonstrates that
520 seaweeds manipulate the composition and connectivity of microbial communities in their
521 proximity. Future study is needed to characterize the metabolites through which the host
522 achieves this and develop a mechanistic understanding of how seaweed biofilm is shaped by
523 their host.

524

525 **DATA AVAILABILITY**

526 The raw de-multiplexed V4-16S rRNA gene reads and corresponding metadata were deposited
527 in the SRA database under the BioProject accession number (PRJNA1180617). Environmental
528 data for temperature and salinity during the given period is available in PANGAEA
529 (<https://doi.org/10.1594/PANGAEA.963281>) [80], and the average values of other
530 environmental data (irradiation, oxygen, salinity) are available in the metadata file (Tab.S1).
531 Scripts for analysis and figures are available via [https://github.com/Marjan-Ghotbi/Seaweeds-](https://github.com/Marjan-Ghotbi/Seaweeds-Microbial-dynamics)
532 [Microbial-dynamics](https://github.com/Marjan-Ghotbi/Seaweeds-Microbial-dynamics).

533

534

535 **AUTHOR CONTRIBUTIONS**

536 MaG and FW conceptualized the study. Field collection, experiments, and laboratory work
537 were conducted by MaG, with supervision from FW. Data processing and analysis were carried
538 out by MaG, with supervision from DMN, and FW. MiG and GB provided valuable input

539 regarding statistical analysis. All authors contributed to the writing and revision of the
540 manuscript.

541

542 **ACKNOWLEDGEMENTS**

543 This study was funded in part by GEOMAR institutional funding received by Martin Wahl and
544 FW, who supported the setup construction, supplies, and materials. Further support was
545 provided by a Young Investigator grant awarded to DMN. We are especially grateful to Martin
546 Wahl for his instrumental role in the experimental design and conceptualization of the study.
547 Our thanks also go to Nadja Stärck and Björn Buchholz for their invaluable assistance during
548 sample collection and setup construction.

549

550

551 **CONFLICT OF INTEREST**

552 The authors declare that they have no conflict of interest.

553

554

555

556

557

558

559

560

561

562

563

564

565

566

567

568

569

570

571

572

573

574

575 REFERENCES

- 576 1. Saha M, Weinberger F. Microbial “gardening” by a seaweed holobiont: Surface
577 metabolites attract protective and deter pathogenic epibacterial settlement. *J Ecol* 2019;
578 **107**: 2255–2265.
- 579 2. van der Loos LM, D’hondt S, Engelen AH, Pavia H, Toth GB, Willems A, et al. Salinity
580 and host drive *Ulva*-associated bacterial communities across the Atlantic-Baltic Sea
581 gradient. *Mol Ecol* 2023; **32**: 6260–6277.
- 582 3. Sharma D, Misba L, Khan AU. Antibiotics versus biofilm: an emerging battleground in
583 microbial communities. *Antimicrob Resist Infect Control* 2019; **8**: 76.
- 584 4. Lazarus E, Meyer AS, Ikuma K, Rivero IV. Three dimensional printed biofilms:
585 Fabrication, design and future biomedical and environmental applications. *Microb*
586 *Biotechnol* 2024; **17**: e14360.
- 587 5. Steinberg PD, de Nys R, Kjelleberg S, Others. Chemical mediation of surface colonization.
588 *Marine chemical ecology CRC Press, Boca Raton, FL* 2001; 355–387.
- 589 6. Lachnit T, Blümel M, Imhoff JF, Wahl M. Specific epibacterial communities on
590 macroalgae: Phylogeny matters more than habitat. *Aquat Biol* 2009; **5**: 181–186.
- 591 7. Aires T, Serrão EA, Engelen AH. Host and environmental specificity in bacterial
592 communities associated to two highly invasive marine species (genus *Asparagopsis*).
593 *Front Microbiol* 2016; **7**.
- 594 8. Kautsky L, Qvarfordt S, Schagerström E. *Fucus vesiculosus* adapted to a life in the Baltic
595 Sea: Impacts on recruitment, growth, re-establishment and restoration. *Botanica Marina*
596 2019; **62**: 17–30.
- 597 9. Hull SL, Scott GW, Johnson LJ. An Investigation of the Genetic Variation in Four Fucales
598 Species Using Cellulose Acetate Electrophoresis. 2001; **44**: 119–123.

- 599 10. Kautskyl N, Kautskyl H, Kautskyl U, Waern M. Decreased depth penetration of *Fucus*
600 *vesiculosus* (L.) since the 1940's indicates eutrophication of the Baltic Sea.
601 <https://www.int-res.com/articles/meps/28/m028p001.pdf>. Accessed 30 Dec 2023.
- 602 11. Lehvo A, Bäck S, Kiirikki M. Growth of *Fucus vesiculosus* L. (Phaeophyta) in the
603 Northern Baltic Proper: Energy and Nitrogen Storage in Seasonal Environment. 2001; **44**:
604 345–350.
- 605 12. Lotze HK, Schramm W. Ecophysiological traits explain species dominance patterns in
606 macroalgal blooms. *J Phycol* 2000; **36**: 287–295.
- 607 13. Isæus M. Factors Structuring *Fucus* Communities at Open and Complex Coastlines in the
608 Baltic Sea. 2004. Stockholm University.
- 609 14. Jueterbock A, Tyberghein L, Verbruggen H, Coyer JA, Olsen JL, Hoarau G. Climate
610 change impact on seaweed meadow distribution in the North Atlantic rocky intertidal. *Ecol*
611 *Evol* 2013; **3**: 1356–1373.
- 612 15. Bellorin AM, Oliveira MC, Oliveira EC. *Gracilaria vermiculophylla*: A western Pacific
613 species of Gracilariaceae (Rhodophyta) first recorded from the eastern Pacific.
614 *Phycological Res* 2004; **52**: 69–79.
- 615 16. Rueness J. Life history and molecular sequences of *Gracilaria vermiculophylla*
616 (*Gracilariales*, Rhodophyta), a new introduction to European waters. *Phycologia* 2005; **44**:
617 120–128.
- 618 17. Thomsen MS, Gurgel CFD, Fredericq S, McGlathery KJ. *Gracilaria vermiculophylla*
619 (Rhodophyta, Gracilariales) in Hog Island bay, Virginia: A cryptic alien and invasive
620 macroalga and taxonomic correction1. *J Phycol* 2006; **42**: 139-41.
- 621 18. Bonthond G, Bayer T, Krueger-Hadfield SA, Barboza FR, Nakaoka M, Valero M, et al.
622 How do microbiota associated with an invasive seaweed vary across scales? *Mol Ecol*
623 2020; **29**: 2094–2108.

- 624 19. Bonthond G, Bayer T, Krueger-Hadfield SA, Stärck N, Wang G, Nakaoka M, et al. The
625 role of host promiscuity in the invasion process of a seaweed holobiont. *ISME J* 2021; 1–
626 12.
- 627 20. Bonthond G, Neu AK, Bayer T, Krueger-Hadfield SA, Künzel S, Weinberger F. Non-
628 native hosts of an invasive seaweed holobiont have more stable microbial communities
629 compared to native hosts in response to thermal stress. *Ecol Evol* 2023; **13**.
- 630 21. Morrissey KL, Çavas L, Willems A, De Clerck O. Disentangling the influence of
631 environment, host specificity and thallus differentiation on bacterial communities in
632 siphonous green seaweeds. *Front Microbiol* 2019; **10**: 717.
- 633 22. Lemay MA, Chen MY, Mazel F, Hind KR, Starko S, Keeling PJ, et al. Morphological
634 complexity affects the diversity of marine microbiomes. *ISME J* 2021; **15**: 1372–1386.
- 635 23. Zhang W, Ding W, Li YX, Tam C, Bougouffa S, Wang R, et al. Marine biofilms constitute
636 a bank of hidden microbial diversity and functional potential. *Nat Commun* 2019; **10**: 1–
637 10.
- 638 24. Debray R, Herbert RA, Jaffe AL, Crits-Christoph A, Power ME, Koskella B. Priority
639 effects in microbiome assembly. *Nat Rev Microbiol* 2022; **20**: 109–121.
- 640 25. Antunes JT, Sousa AGG, Azevedo J, Rego A, Leão PN, Vasconcelos V. Distinct Temporal
641 Succession of Bacterial Communities in Early Marine Biofilms in a Portuguese Atlantic
642 Port. *Front Microbiol* 2020; **11**: 1–17.
- 643 26. Lee OO, Wang Y, Tian R, Zhang W, Shek CS, Bougouffa S, et al. In situ environment
644 rather than substrate type dictates microbial community structure of biofilms in a cold seep
645 system. *Sci Rep* 2014; **4**: 1–10.
- 646 27. Wahl M, Buchholz B, Winde V, Golomb D, Guy-Haim T, Müller J, et al. A mesocosm
647 concept for the simulation of near-natural shallow underwater climates: The Kiel Outdoor
648 Benthocosms (KOB). *Limnol Oceanogr Methods* 2015; **13**: 651–663.

- 649 28. Doyle J. DNA Protocols for Plants. In: Hewitt GM, Johnston AWB, Young JPW (eds).
650 *Molecular Techniques in Taxonomy*. 1991. Springer Berlin Heidelberg, Berlin,
651 Heidelberg, pp 283–293.
- 652 29. Gohl DM, Vangay P, Garbe J, Maclean A, Hauge A, Becker A, et al. Systematic
653 improvement of amplicon marker gene methods for increased accuracy in microbiome
654 studies. *Nat Biotechnol* 2016; 1–11.
- 655 30. Martin M. Cutadapt removes adapter sequences from high-throughput sequencing reads.
656 *EMBnet J* 2011; **17**: 10.
- 657 31. Callahan BJ, McMurdie PJ, Rosen MJ, Han AW, Johnson AJA, Holmes SP. DADA2:
658 High-resolution sample inference from Illumina amplicon data. *Nat Methods* 2016; **13**:
659 581–583.
- 660 32. Bolyen E, Rideout JR, Dillon MR, Bokulich NA, Abnet CC, Al-Ghalith GA, et al.
661 Reproducible, interactive, scalable and extensible microbiome data science using QIIME
662 2. *Nat Biotechnol* 2019; **37**: 852–857.
- 663 33. Bokulich NA, Kaehler BD, Rideout JR, Dillon M, Bolyen E, Knight R, et al. Optimizing
664 taxonomic classification of marker-gene amplicon sequences with QIIME 2’s q2-feature-
665 classifier plugin. *Microbiome* 2018; **6**: 90.
- 666 34. Yilmaz P, Parfrey LW, Yarza P, Gerken J, Pruesse E, Quast C, et al. The SILVA and “All-
667 species Living Tree Project (LTP)” taxonomic frameworks. *Nucleic Acids Res* 2013; **42**:
668 D643–D648.
- 669 35. Stoddard SF, Smith BJ, Hein R, Roller BRK, Schmidt TM. rrnDB: improved tools for
670 interpreting rRNA gene abundance in bacteria and archaea and a new foundation for future
671 development. *Nucleic Acids Res* 2015; **43**: D593-8.
- 672 36. Chen MY, Chen JW, Wu LW, Huang KC, Chen JY, Wu WS, et al. Carcinogenesis of Male
673 Oral Submucous Fibrosis Alters Salivary Microbiomes. *J Dent Res* 2021; **100**: 397–405.

- 674 37. Decelle J, Romac S, Stern RF, Bendif EM, Zingone A, Audic S, et al. PhytoREF: A
675 reference database of the plastidial 16S rRNA gene of photosynthetic eukaryotes with
676 curated taxonomy. *Mol Ecol Resour* 2015; **15**: 1435–1445.
- 677 38. Needham DM, Fuhrman JA. Pronounced daily succession of phytoplankton, archaea and
678 bacteria following a spring bloom. *Nature microbiology* 2016; **1**: 16005.
- 679 39. Neu AT. Defining and quantifying the core microbiome : Challenges and prospects. 2021;
680 **118**: 1–10.
- 681 40. Risely A. Applying the core microbiome to understand host–microbe systems. *J Anim Ecol*
682 2020; **89**: 1549–1558.
- 683 41. Shade A, Handelsman J. Minireview Beyond the Venn diagram : the hunt for a core
684 microbiome. 2012; **14**: 4–12.
- 685 42. Jones SE, Lennon JT. Dormancy contributes to the maintenance of microbial diversity.
686 *Proc Natl Acad Sci U S A* 2010; **107**: 5881–5886.
- 687 43. Kurtz ZD, Müller CL, Miraldi ER, Littman DR, Blaser MJ, Bonneau RA. Sparse and
688 Compositionally Robust Inference of Microbial Ecological Networks. *PLoS Comput Biol*
689 2015; **11**: 1–25.
- 690 44. Deng Y, Jiang Y-H, Yang Y, He Z, Luo F, Zhou J. Molecular ecological network analyses.
691 2012.
- 692 45. Ghotbi M, Ghotbi M, Kuzyakov Y, Horwath WR. Management and rhizosphere microbial
693 associations modulate genetic-driven nitrogen fate. *Agric Ecosyst Environ* 2025; **378**:
694 109308.
- 695 46. Ghotbi M, Taghizadeh-Mehrjardi R, Knief C, Ghotbi M, Kent AD, Horwath WR. The
696 patchiness of soil ¹³C versus the uniformity of ¹⁵N distribution with geomorphic position
697 provides evidence of erosion and accelerated organic matter turnover. *Agric Ecosyst*
698 *Environ* 2023; **356**: 108616.

- 699 47. R-project. org/package= vegan H, 2011. vegan: Community Ecology Package-R package
700 version 1.17-8. *cir.nii.ac.jp* 2011.
- 701 48. Lin H, Peddada SD. Analysis of compositions of microbiomes with bias correction. *Nat*
702 *Commun* 2020; **11**: 3514.
- 703 49. Peng G-S, Tan S-Y, Wu J, Holme P. Trade-offs between robustness and small-world effect
704 in complex networks. *Sci Rep* 2016; **6**: 37317.
- 705 50. Guo B, Zhang L, Sun H, Gao M, Yu N, Zhang Q, et al. Microbial co-occurrence network
706 topological properties link with reactor parameters and reveal importance of low-
707 abundance genera. *npj Biofilms and Microbiomes* 2022; **8**: 1–13.
- 708 51. Vargas-Gastélum L, Romer AS, Ghotbi M, Dallas JW, Alexander NR, Moe KC, et al.
709 Herptile gut microbiomes: a natural system to study multi-kingdom interactions between
710 filamentous fungi and bacteria. *mSphere* 2024; e0047523.
- 711 52. Liu X, Li M, Castelle CJ, Probst AJ, Zhou Z, Pan J, et al. Insights into the ecology,
712 evolution, and metabolism of the widespread Woese archaeotal lineages. *Microbiome*
713 2018; **6**: 102.
- 714 53. Castelle CJ, Wrighton KC, Thomas BC, Hug LA, Brown CT, Wilkins MJ, et al. Genomic
715 Expansion of Domain Archaea Highlights Roles for Organisms from New Phyla in
716 Anaerobic Carbon Cycling. *Curr Biol* 2015; **25**: 690–701.
- 717 54. Huang W-C, Liu Y, Zhang X, Zhang C-J, Zou D, Zheng S, et al. Comparative genomic
718 analysis reveals metabolic flexibility of Woese archaeota. *Nat Commun* 2021; **12**: 1–14.
- 719 55. Agler MT, Ruhe J, Kroll S, Morhenn C, Kim ST, Weigel D, et al. Microbial Hub Taxa
720 Link Host and Abiotic Factors to Plant Microbiome Variation. *PLoS Biol* 2016; **14**: 1–31.
- 721 56. Jens M. Olesen*† JBYLDAPJ. The modularity of pollination networks. 2007. PNAS.
- 722 57. Pei P, Aslam M, Du H, Liang H, Wang H, Liu X, et al. Environmental factors shape the
723 epiphytic bacterial communities of *Gracilaria lemaneiformis*. *Sci Rep* 2021; **11**: 1–15.

- 724 58. Comba González NB, Niño Corredor AN, López Kleine L, Montoya Castaño D. Temporal
725 Changes of the Epiphytic Bacteria Community From the Marine Macroalga *Ulva lactuca*
726 (Santa Marta, Colombian-Caribbean). *Curr Microbiol* 2021; **78**: 534–543.
- 727 59. Mudlaff CM, Weinberger F, Düsedau L, Ghotbi M, Künzel S, Bonthond G. Seasonal
728 cycles in a seaweed holobiont: A multiyear time series reveals repetitive microbial shifts
729 and core taxa. *bioRxiv* . 2024. , 2024.10. 23.619769
- 730 60. Amin SA, Parker MS, Armbrust EV. Interactions between Diatoms and Bacteria.
731 *Microbiol Mol Biol Rev* 2012; **76**: 667–684.
- 732 61. Dang Hongyue, Li Tiegang, Chen Mingna, Huang Guiqiao. Cross-Ocean Distribution of
733 Rhodobacterales Bacteria as Primary Surface Colonizers in Temperate Coastal Marine
734 Waters. *Appl Environ Microbiol* 2008; **74**: 52–60.
- 735 62. Kang I, Lim Y, Cho J-C. Complete genome sequence of *Granulosicoccus antarcticus* type
736 strain IMCC3135T, a marine gammaproteobacterium with a putative
737 dimethylsulfoniopropionate demethylase gene. *Mar Genomics* 2018; **37**: 176–181.
- 738 63. Nowinski B, Motard-Côté J, Landa M, Preston CM, Scholin CA, Birch JM, et al.
739 Microdiversity and temporal dynamics of marine bacterial dimethylsulfoniopropionate
740 genes. *Environ Microbiol* 2019; **21**: 1687–1701.
- 741 64. Weigel Brooke L., Miranda Khashiff K., Fogarty Emily C., Watson Andrea R., Pfister
742 Catherine A. Functional Insights into the Kelp Microbiome from Metagenome-Assembled
743 Genomes. *mSystems* 2022; **7**: e01422-21.
- 744 65. Levine JM, HilleRisLambers J. The importance of niches for the maintenance of species
745 diversity. *Nature* 2009; **461**: 254–257.
- 746 66. Song J, Hwang J, Kang I, Cho J-C. A sulfate-reducing bacterial genus,
747 *Desulfosediminicola* gen. nov., comprising two novel species cultivated from tidal-flat
748 sediments. *Sci Rep* 2021; **11**: 19978.

- 749 67. Shaw DK, Sekar J, Ramalingam PV. Recent insights into oceanic
750 dimethylsulfoniopropionate biosynthesis and catabolism. *Environ Microbiol* 2022; **24**:
751 2669–2700.
- 752 68. Dang H, Lovell CR. Microbial Surface Colonization and Biofilm Development in Marine
753 Environments. *Microbiol Mol Biol Rev* 2016; **80**: 91–138.
- 754 69. Williams TJ, Allen MA, Berengut JF, Cavicchioli R. Shedding Light on Microbial “Dark
755 Matter”: Insights Into Novel Cloacimonadota and Omnitrophota From an Antarctic Lake.
756 *Front Microbiol* 2021; **12**: 741077.
- 757 70. Tsola SL, Zhu Y, Ghurnee O, Economou CK, Trimmer M, Eyice Ö. Diversity of
758 dimethylsulfide-degrading methanogens and sulfate-reducing bacteria in anoxic sediments
759 along the Medway Estuary, UK. *Environ Microbiol* 2021; **23**: 4434–4449.
- 760 71. Zou D, Zhang C, Liu Y, Li M. Biogeographical distribution and community assembly of
761 Myxococcota in mangrove sediments. *Environ Microbiome* 2024; **19**: 47.
- 762 72. Rosales SM, Miller MW, Williams DE, Traylor-Knowles N, Young B, Serrano XM.
763 Microbiome differences in disease-resistant vs. susceptible *Acropora* corals subjected to
764 disease challenge assays. *Sci Rep* 2019; **9**: 18279.
- 765 73. Kopprio GA, Cuong LH, Luyen ND, Duc TM, Ha TH, Huong LM, et al. Carrageenophyte-
766 attached and planktonic bacterial communities in two distinct bays of Vietnam:
767 Eutrophication indicators and insights on ice-ice disease. *Ecol Indic* 2021; **121**: 107067.
- 768 74. Beiralas R, Ozer N, Segev E. Abundant Sulfitobacter marine bacteria protect *Emiliania*
769 *huxleyi* algae from pathogenic bacteria. *ISME Communications* 2023; **3**: 1–10.
- 770 75. Lin S, Guo Y, Huang Z, Tang K, Wang X. Comparative Genomic Analysis of Cold-Water
771 Coral-Derived *Sulfitobacter faviae*: Insights into Their Habitat Adaptation and
772 Metabolism. *Mar Drugs* 2023; **21**.

- 773 76. Li B, Lu F, Wei X, Zhao R. Fucoidan: structure and bioactivity. *Molecules* 2008; **13**: 1671–
774 1695.
- 775 77. Lage OM, Bondoso J. Planctomycetes and macroalgae, a striking association. *Front*
776 *Microbiol* 2014; **5**: 267.
- 777 78. Phooprong S, Ogawa H, Hayashizaki K. Photosynthetic and respiratory responses of
778 *Gracilaria vermiculophylla* (Ohmi) Papenfuss collected from Kumamoto, Shizuoka and
779 Iwate, Japan. *J Appl Phycol* 2008; **20**: 743–750.
- 780 79. Klock MM, Barrett LG, Thrall PH, Harms KE. Host promiscuity in symbiont associations
781 can influence exotic legume establishment and colonization of novel ranges. *Divers*
782 *Distrib* 2015; **21**: 1193–1203.
- 783 80. Hiebenthal C, Begler C, Melzner F. Continuous water temperature and salinity data in
784 front of GEOMAR Pier, Kiel, Germany (2022-2023). 2023. PANGAEA.
- 785
786
787
788
789
790
791
792
793
794
795
796
797

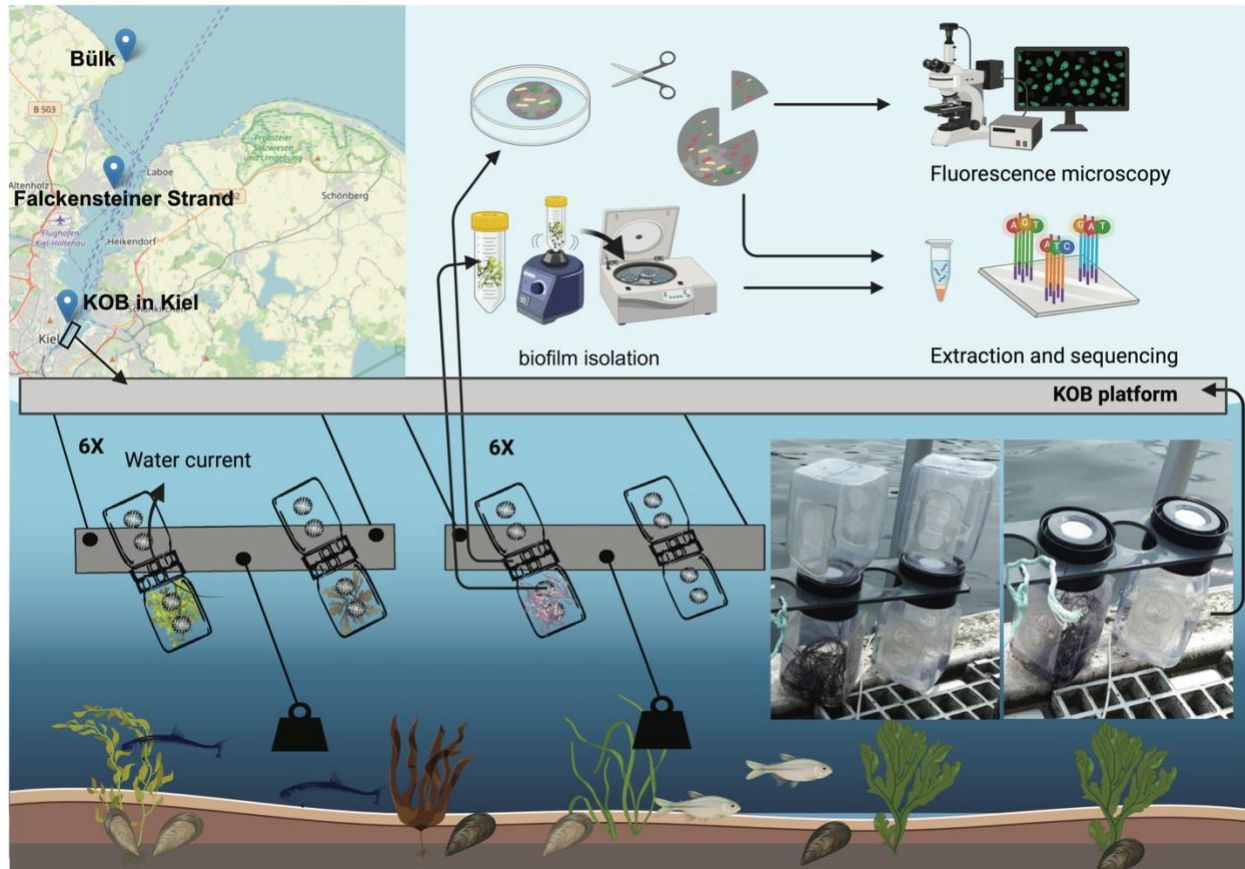


Fig.1. EXUTAX composed of 12 panels (plus one control panel for observation), each carrying two double-attached 1 l kautex bottles with a circular washer, as a place holder for polycarbonate filters, connecting them. Kautex bottles had four mesh-covered holes (diameter: 20 mm) on two opposing sides, allowing a current of seawater pass through constantly. The washer had a channel (diameter: 5 mm) in the middle connecting the flow between attached bottles. Seaweed specimens were deposited in individual kautex bottles, connected to an empty bottle which was harbouring the polycarbonate filter. Seaweed species and control empty bottles were arranged randomly in six replicates among panels. The whole EXUTAX was submerged in the Kiel Fjord, hanging from KOB platform, at the depth of approximately 50 cm. The set up was maintained perpendicularly by adjustment of weights to avoid sedimentation on filters. Arrangement of mesh-covered holes on two opposing sides of bottles along with the connecting channel between them allowed a current of seawater in contact with algal exudates pass through filters constantly.

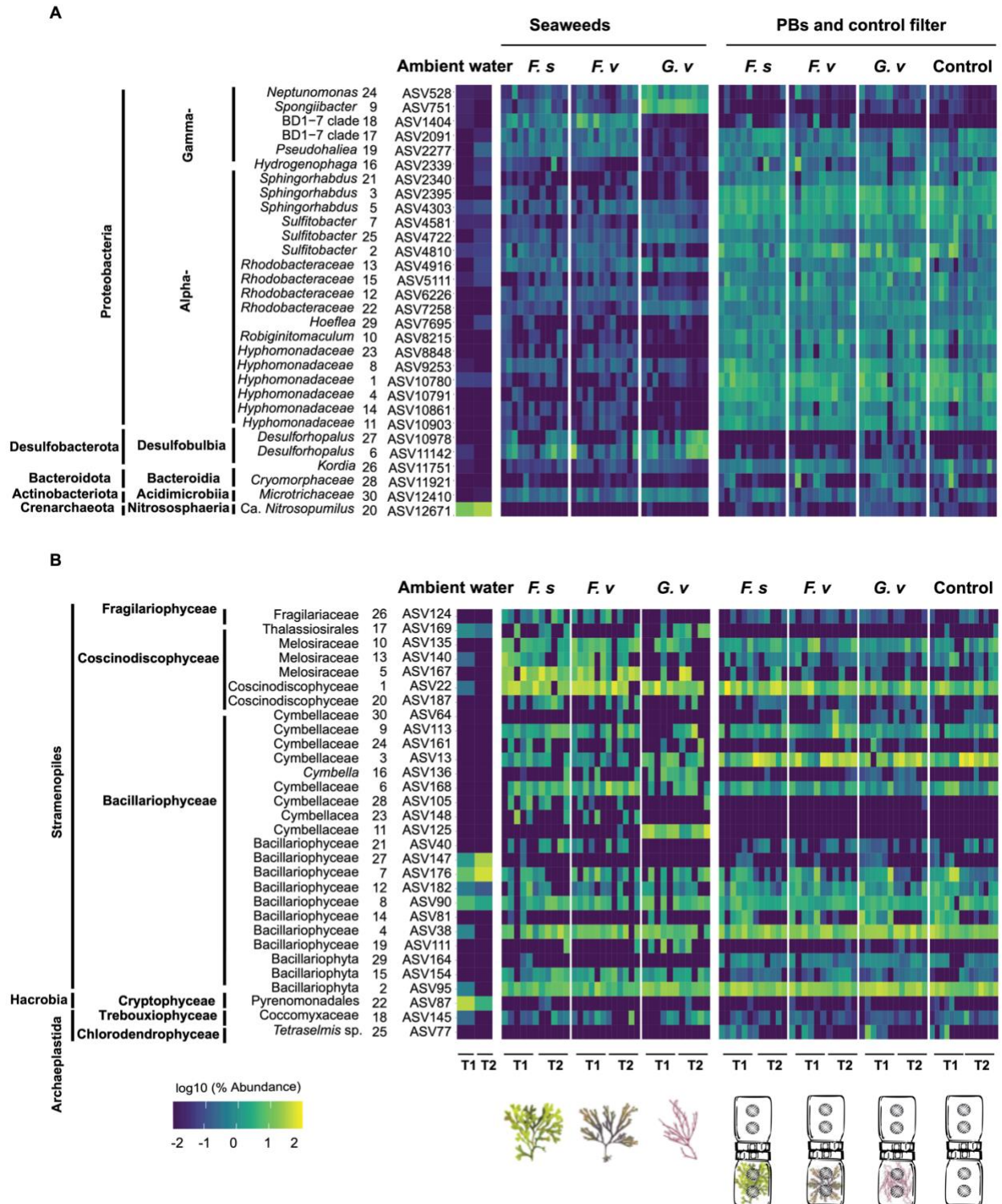


Fig.2. Heatmap representing the top 30 most abundant A) Prokaryotic and B) Microalgae ASVs during two experiments. Each sample group (seaweeds, PBs and control) has six replicates in each timepoint except for ambient seawater with two replicates and controls with one additional

replicate). ASVs are classified at their highest detected resolution. The numbers printed on the lefthand side of ASV codes represents their order in relative abundance, with 1 being the most abundant ASV. The relative abundance of ASVs is log10 transformed. Seaweed and filter sample illustrations are shown below the heatmap for reference.

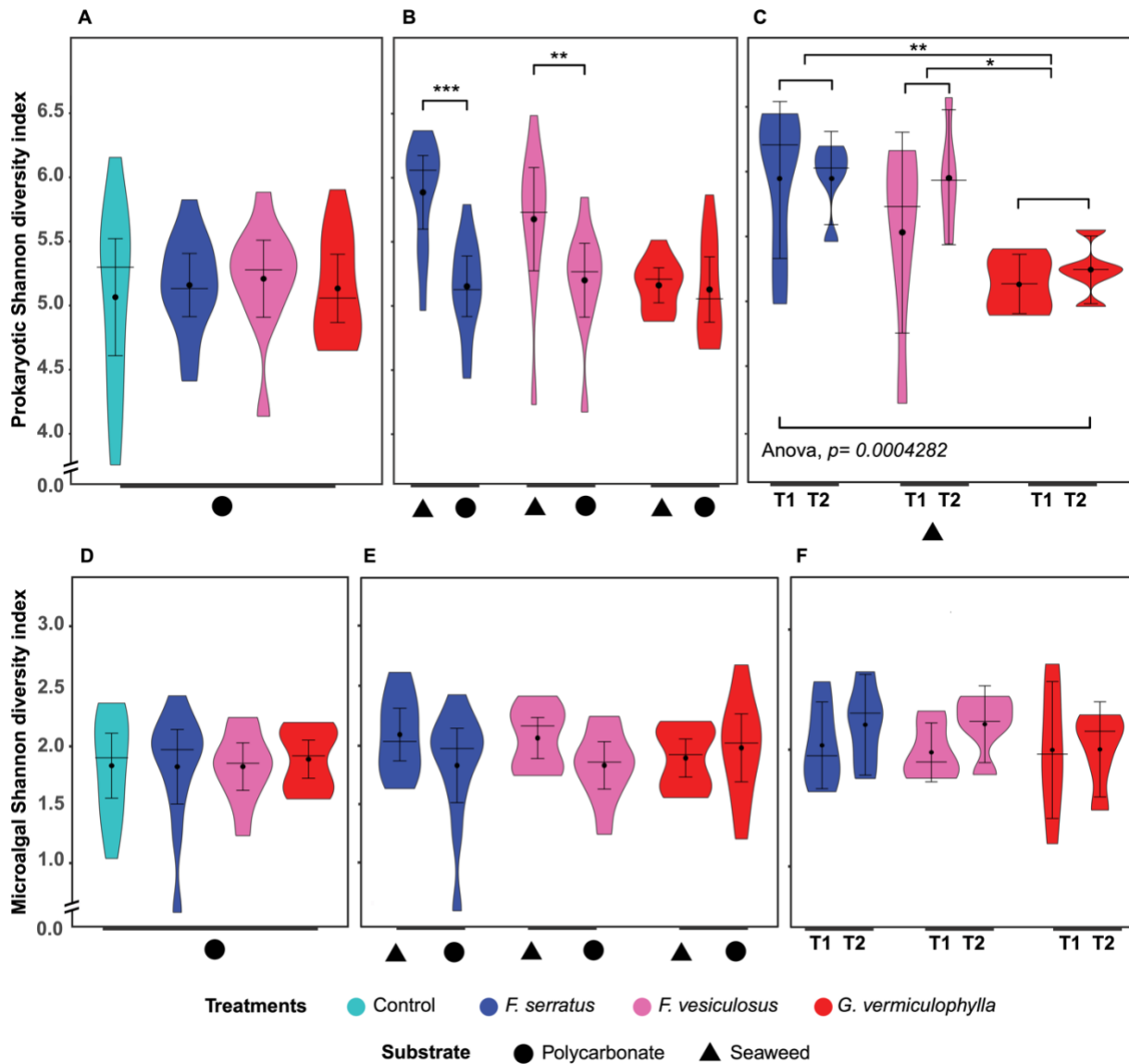


Fig.3. Diversity (α -diversity) of A) Prokaryotes and B) Microalgae for different samples on living (seaweeds) and non-living (polycarbonate) substrate types over two experiments. Violin plots showing median, interquartile range (with outliers) and the point and the bar showing the mean and the standard deviation. Six replicates at each timepoint were used for different treatments.

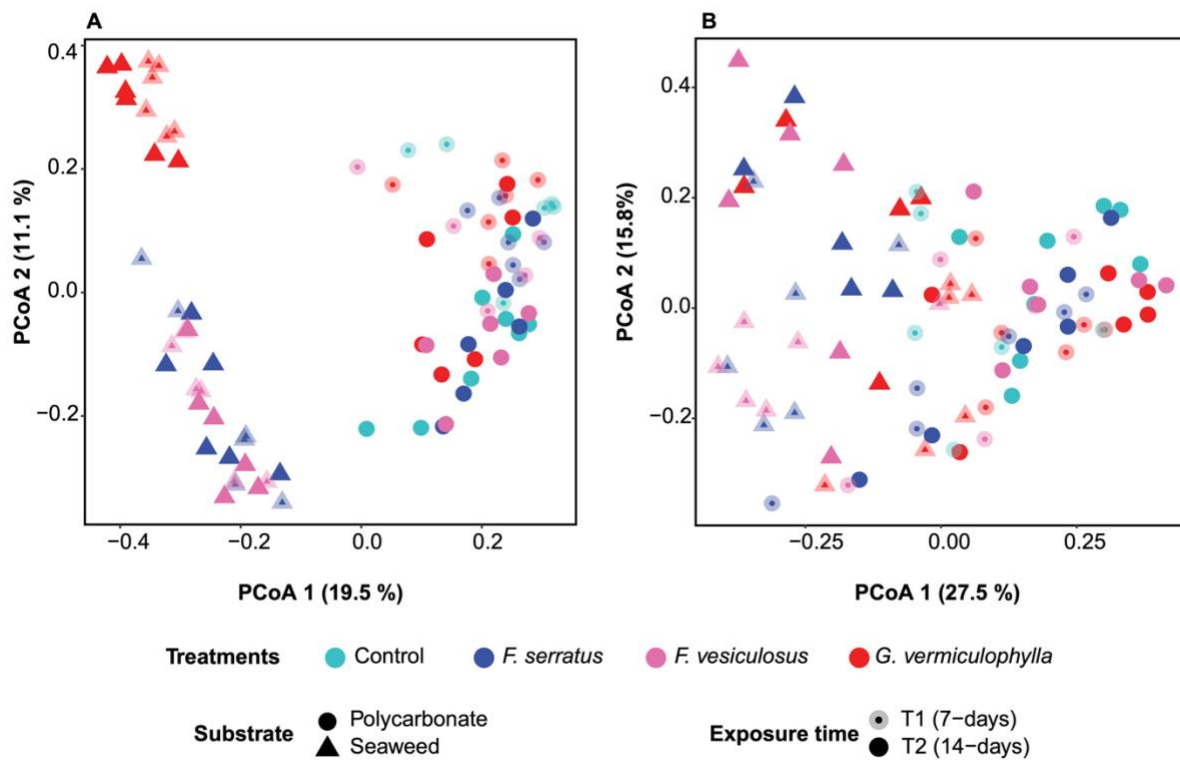


Fig.4. PCoA plots demonstrating A) Prokaryotes and B) Microalgae community clustering based on Bray-Curtis dissimilarity matrices. The number of replicates for sample groups for each experiment was six, except for controls with seven replicates.

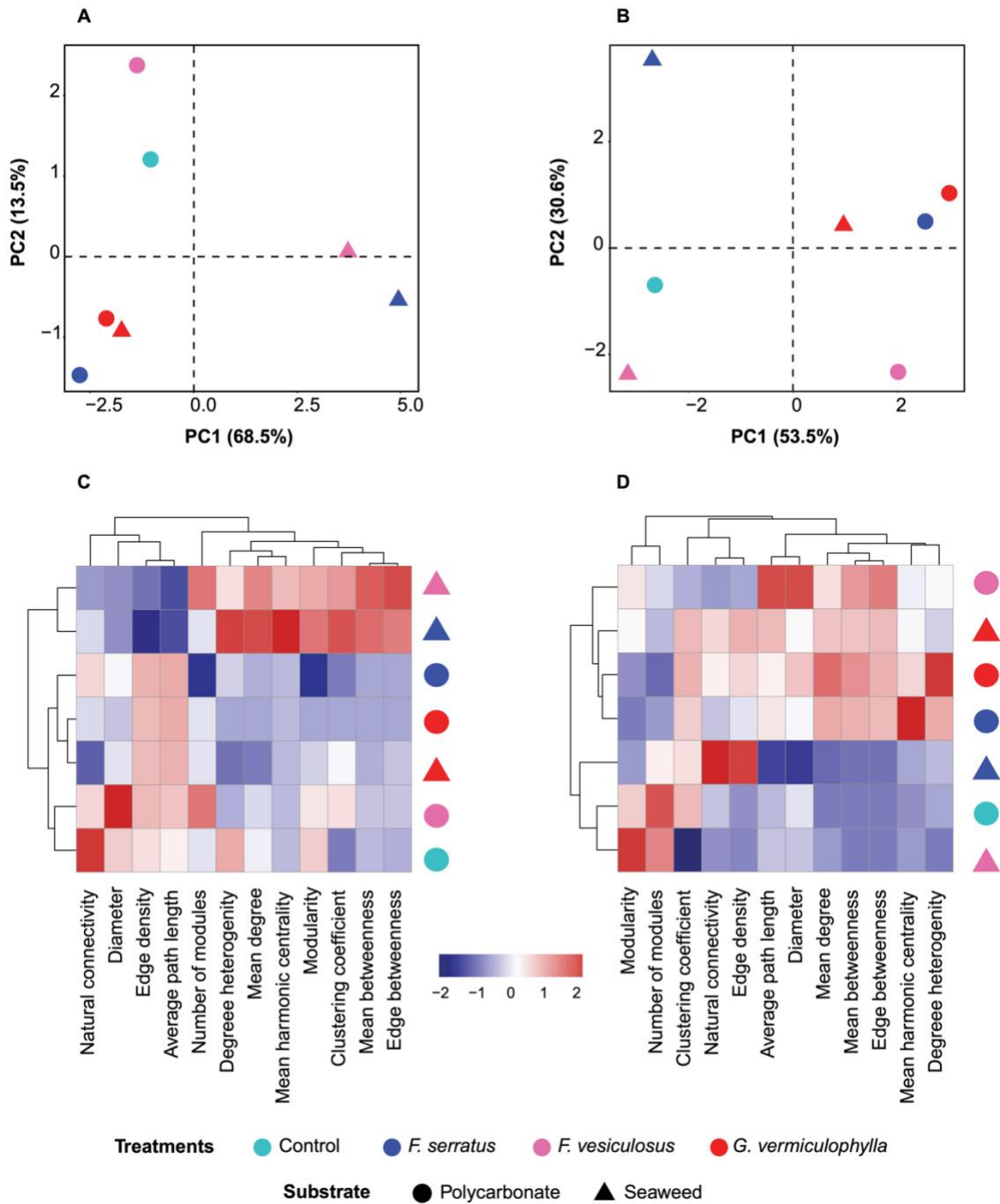


Fig.5. PCA plot where distances represent the dissimilarity between microbial association networks of A) whole microbial community (WMC: > 0.25% relative abundance) and B) core microbiomes (≥ 90 prevalence) of seaweed biofilms and their PBs and control. Heatmaps comparing network variables for C) WMC vs. D) core microbiomes of the corresponding samples.

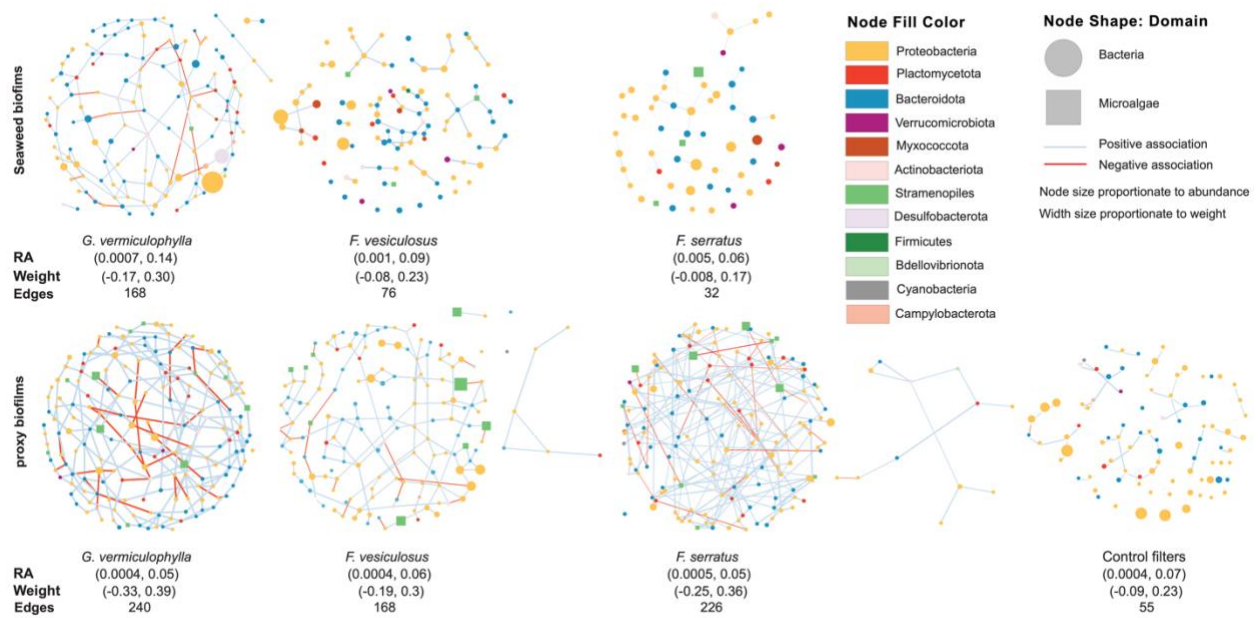


Fig.6. Microbial association networks of core microbiomes of algae and PBs including bacteria and microalgae. Each node represents an ASV and is shaped according to the taxonomic domain. Edge color denotes a positive (blue) or negative (red) association between two connected ASVs with the width proportional to weight (correlation coefficient of nodes abundances representing strength of associations). The corresponding maximum and minimum values for RA (Relative Abundance) and weight, and number of edges are provided underneath each network plot. Generally, the highest number of associations are seen in the networks of *G. vermiculophylla* among both seaweeds and PBs.

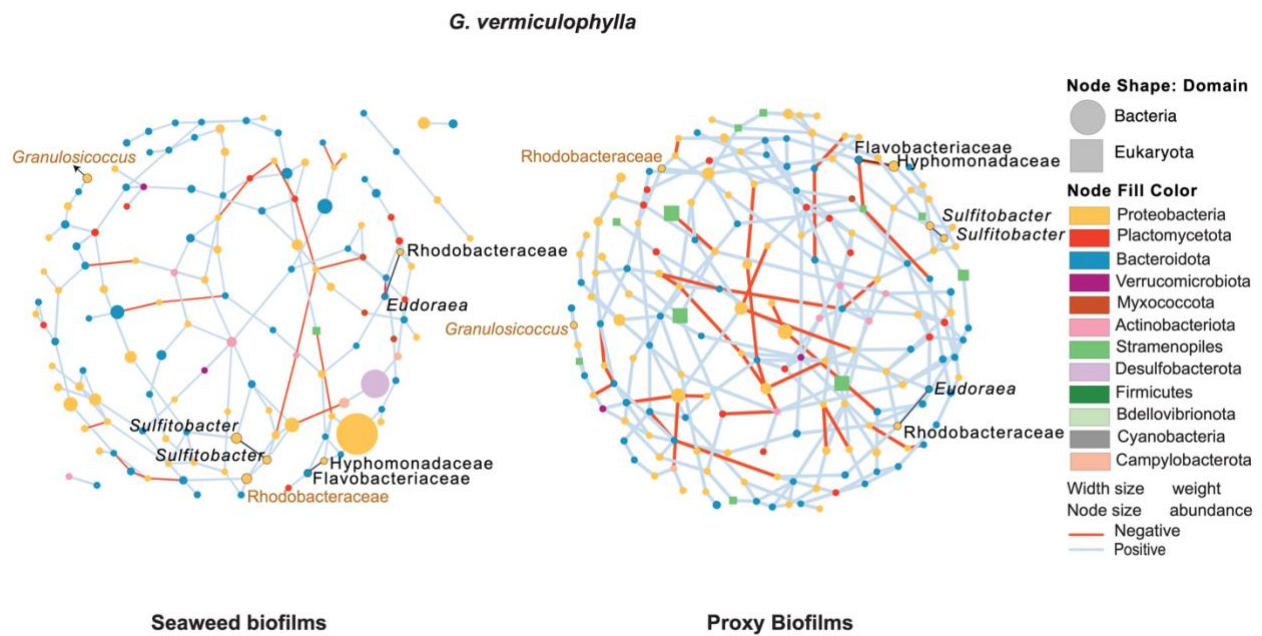


Fig.7. Comparison of microbial association networks in *G. vermiculophylla* seaweed and its PB with 46 nodes (ASVs) and three associations (edges in black) shared between them. Node shape represents microbial domain and node color shows their phyla. Edge color indicates a positive (blue) or negative (red) association and the edge width is proportional to weight. Two ASVs in brown color are hosts-specific taxa exclusively shared between *G. vermiculophylla* and its PBs.